Supporting Information

Humidity and Ultra-violet Modulate Color Turned LnNa-based Metal-Organic Frameworks as Bi-decryption Anti-counterfeit Materials

Jinzeng Wang[a], Mengjuan Cui[a], Haiyun Yao[b], Fang Wang*[a], Xiaolong Li*[a]*

J. Z. Wang, M. J. Cui, F. Wang, X. L. Li

Key Laboratory of Magnetic Molecules & Magnetic Information Materials Ministry of Education, School of Chemistry & Material Science, Shanxi Normal University Taiyuan 030031, Shanxi Province, China

E-mail: jinzenggd@163.com

H. Y. Yao

School of Opto-electronic Engineering, Zaozhuang University, Zaozhuang 277160, Shandong Province, China

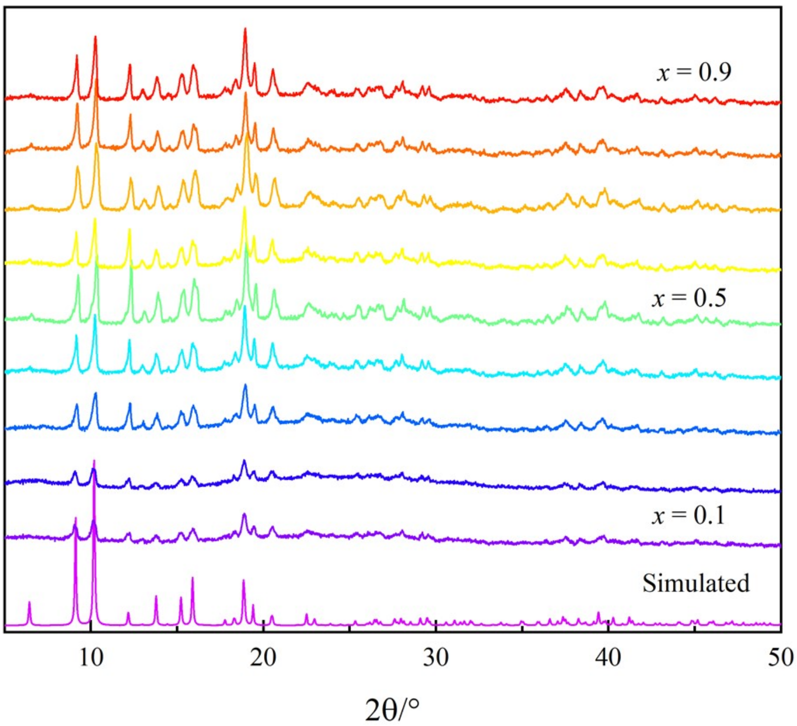

Fig. S1 Experimental powder X-ray diffraction diagrams of $Gd_{1-x}Tb_xHIP$ ($0 \le x \le 1$, step 0.1) and simulated PXRD

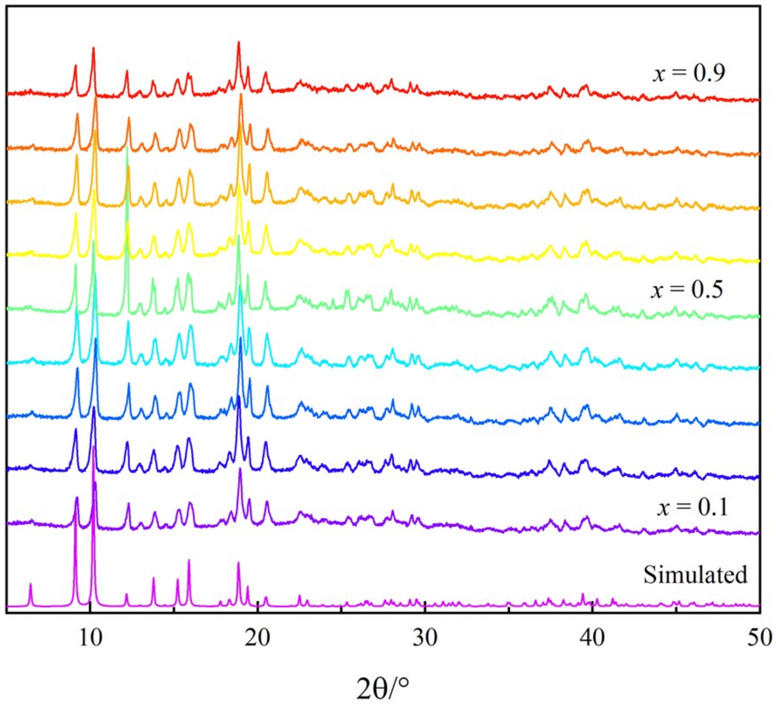

Fig. S2 Experimental powder X-ray diffraction diagrams of $Gd_{1-x}Eu_xHIP$ (0 ≤ x ≤ 1, step 0.1) and simulated PXRD

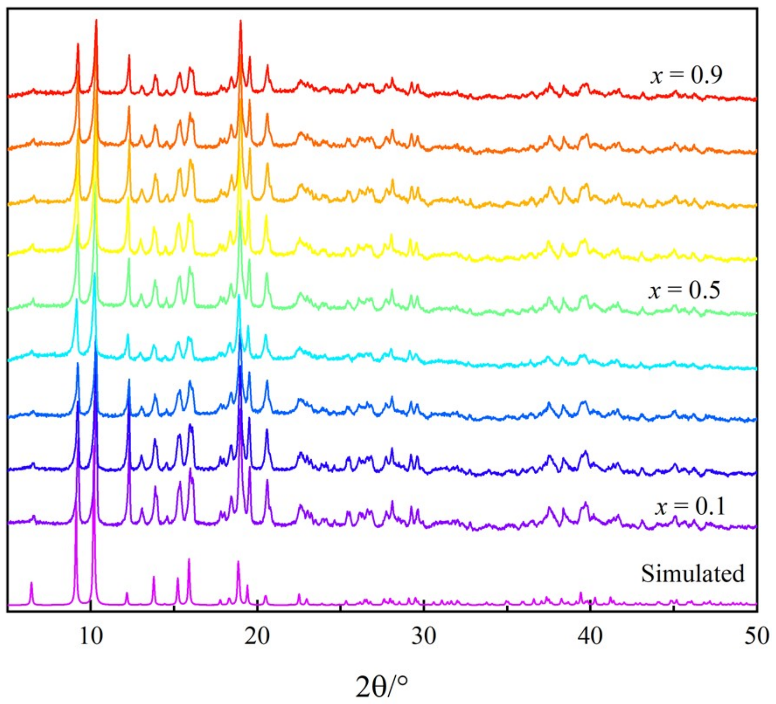

Fig. S3 Experimental powder X-ray diffraction diagrams of $Gd_{0.5}Tb_{0.5x}Eu_{0.5-0.5x}HIP$ (0 ≤ x ≤ 1, step 0.1) and simulated PXRD

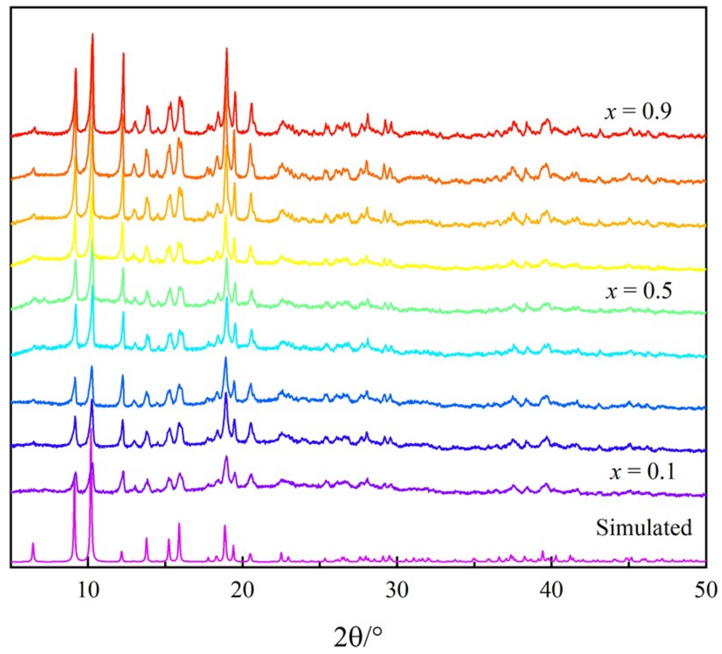

Fig. S4 Experimental powder X-ray diffraction diagrams of $Gd_{1-x}Dy_xHIP$ ($0 \le x \le 1$, step 0.1) and simulated PXRD

Table S1 Relative metallic content measured by EDS for the molecular alloys of $Gd_{1-x}Tb_xHIP$, $Gd_{1-x}Eu_xHIP$ ($0 \le x \le 1$, step 0.1)

$Gd_{1-x}Tb_xHIP$			$Gd_{1-x}Eu_xHIP$		
x	Gd %	Tb %	x	Gd %	Eu %
0.1	91(2)	9(2)	0.1	91(2)	9(2)
0.2	81(2)	19(2)	0.2	82(2)	18(2)
0.3	70(2)	30(2)	0.3	72(2)	28(2)
0.4	60(2)	40(2)	0.4	61(2)	39(2)
0.5	50(2)	50(2)	0.5	50(2)	50(2)
0.6	40(2)	60(2)	0.6	59(2)	41(2)
0.7	29(2)	71(2)	0.7	70(2)	30(2)
0.8	18(2)	82(2)	0.8	80(2)	20(2)
0.9	9 (2)	91(2)	0.9	90 (2)	10(2)

Table S2 Relative metallic content measured by EDS for the molecular alloys of $Gd_{0.5}Tb_{0.5x}Eu_{0.5-0.5x}HIP$, $Gd_{1-x}Dy_xHIP$ ($0 \le x \le 1$, step 0.1)

$Gd_{1-x}Dy_xHIP$			$Gd_{0.5}Tb_{0.5x}Eu_{0.5-0.5x}HIP$			
x	Gd %	Dy %	x	Gd %	Tb %	Eu
0.1	92(2)	8(2)	0.1	50(2)	4(2)	46(2)
0.2	81(2)	19(2)	0.2	50(2)	9(2)	41(2)
0.3	71(2)	29(2)	0.3	50(2)	14(2)	36(2)
0.4	62(2)	38(2)	0.4	50(2)	19(2)	31(2)
0.5	50(2)	50(2)	0.5	50(2)	25(2)	25(2)
0.6	41(2)	59(2)	0.6	50(2)	30(2)	20(2)
0.7	31(2)	69(2)	0.7	50(2)	34(2)	16(2)
0.8	21(2)	79(2)	0.8	50(2)	40(2)	10(2)
0.9	11(2)	89(2)	0.9	50(2)	46(2)	4(2)

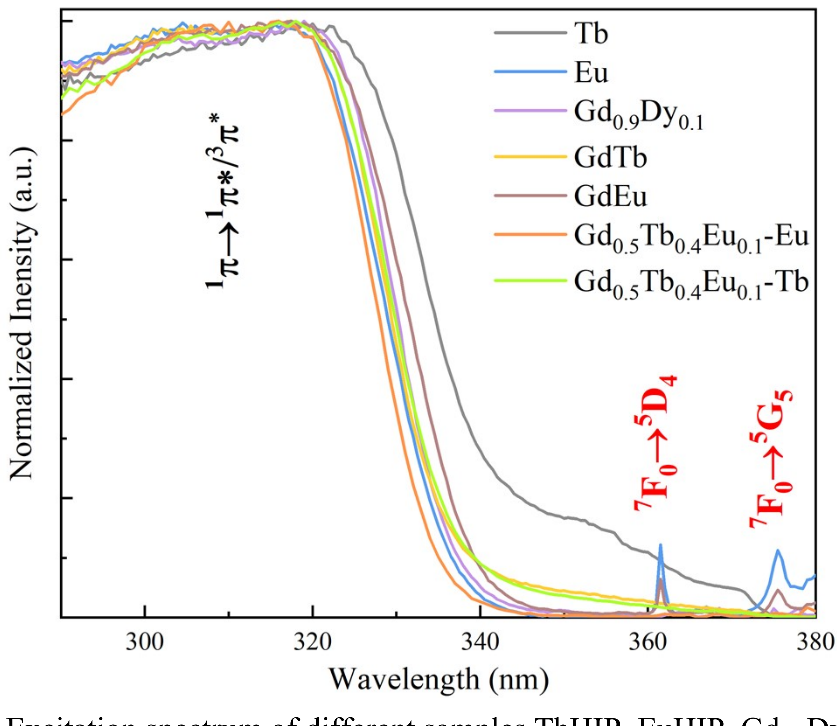

Fig. S5 Excitation spectrum of different samples TbHIP, EuHIP, $Gd_{0.9}Dy_{0.1}HIP$, $Gd_{0.5}Tb_{0.5}HIP$, $Gd_{0.5}Eu_{0.5}HIP$, $Gd_{0.5}Tb_{0.4}Eu_{0.1}HIP$

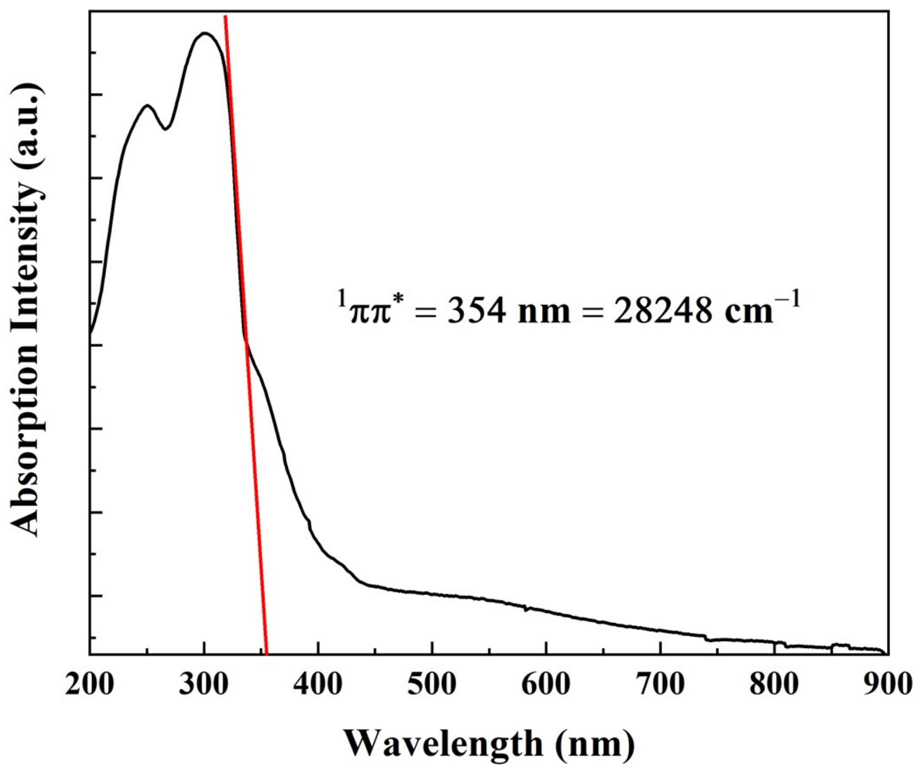

Fig. S6 The solid state absorption spectrum of GdHIP.

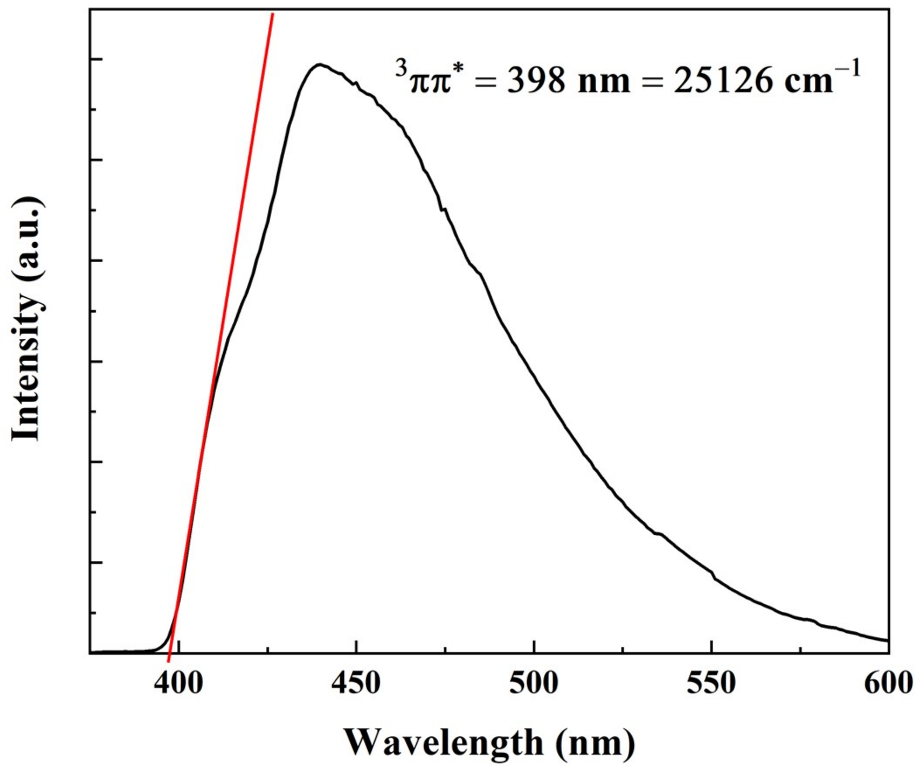

Fig. S7 The emission spectrum of GdHIP at 77 K.

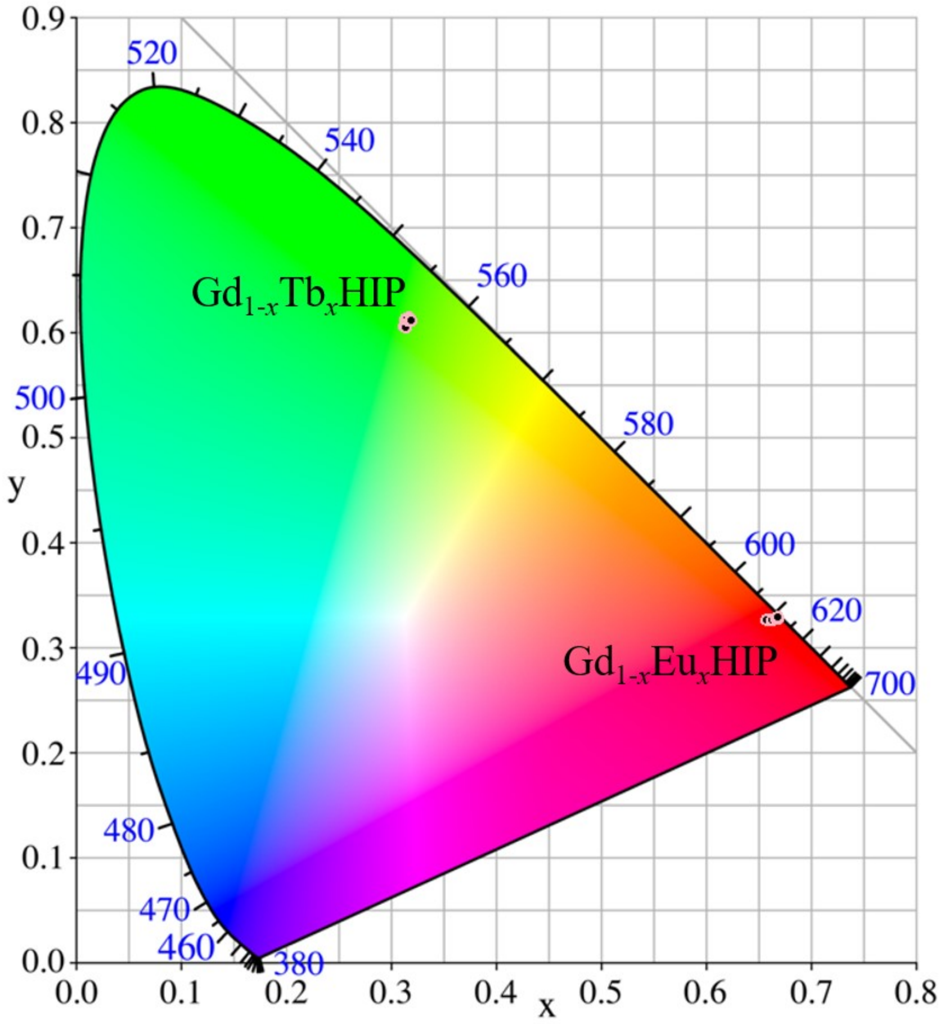

Fig. S8 The CIE coordinates of $Gd_{1-x}Tb_xHIP$ and $Gd_{1-x}Eu_xHIP$ molecular alloys

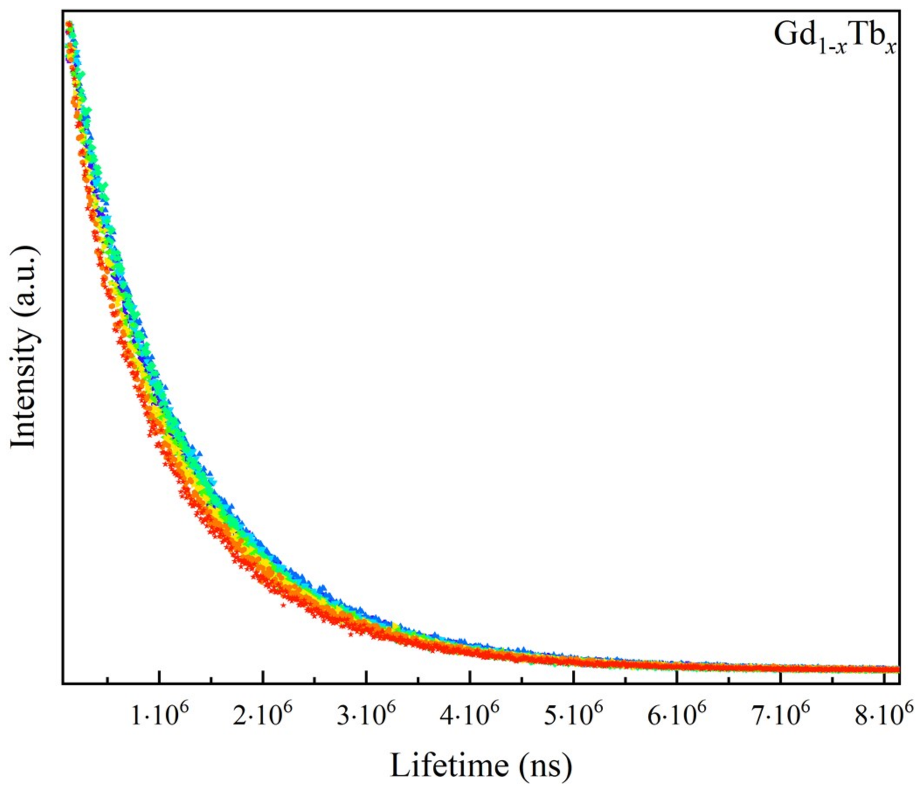

Fig. S9 The luminescent lifetime decay curves of $Gd_{1-x}Tb_x$HIP

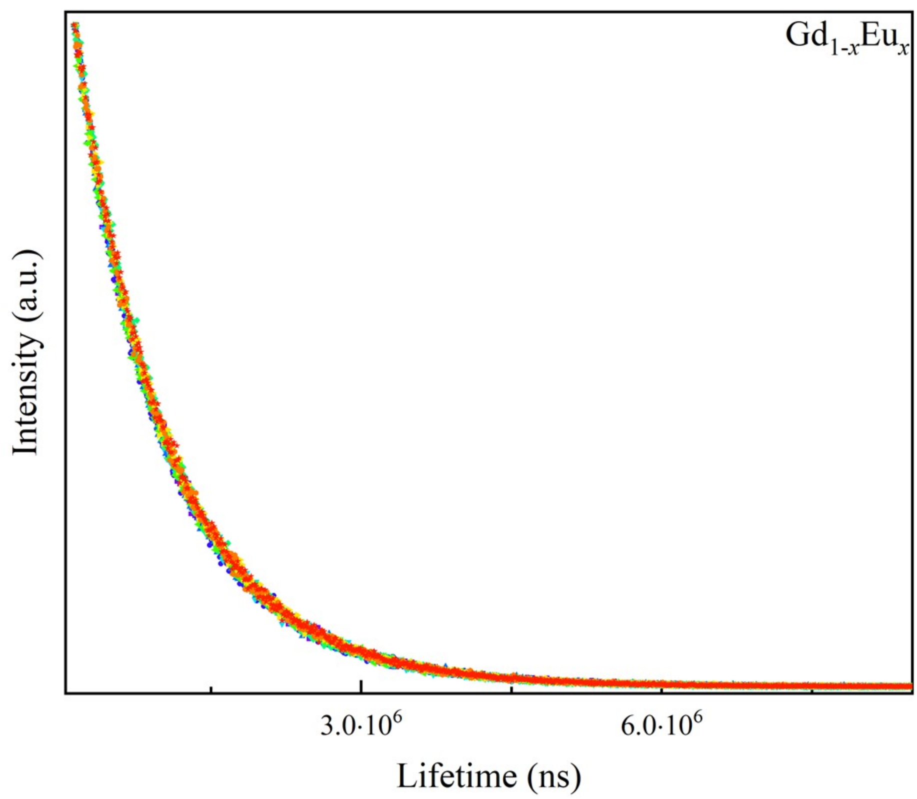

Fig. S10 The luminescent lifetime decay curves of $Gd_{1-x}Eu_x$HIP

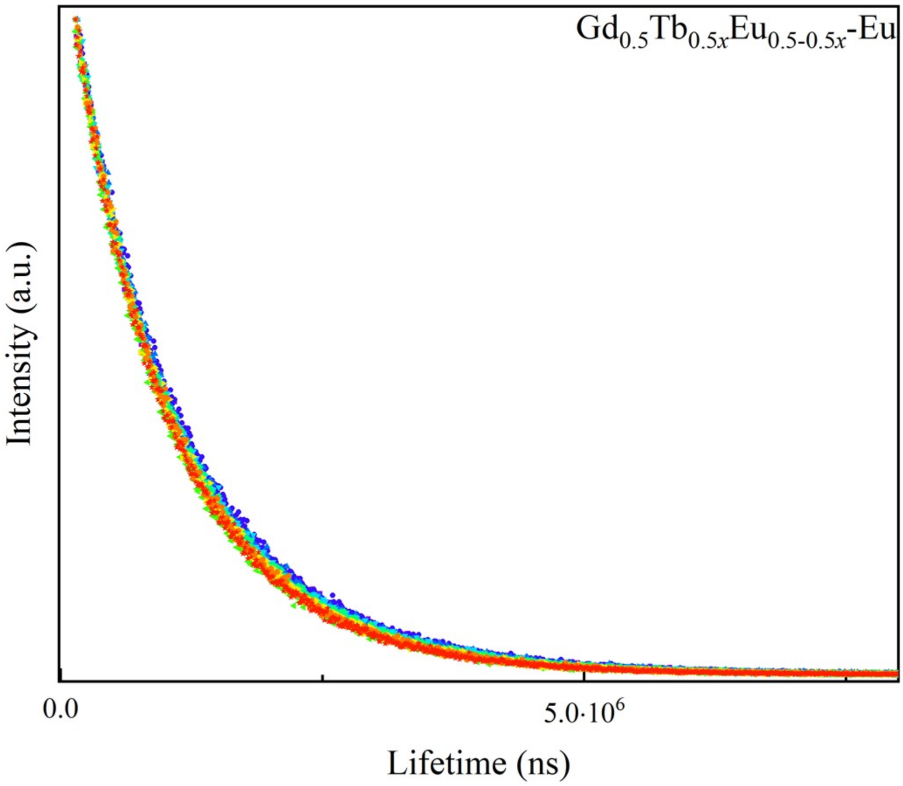

Fig. S11 The luminescent lifetime decay curves of Eu^{3+} for $Gd_{0.5}Tb_{0.5x}Eu_{0.5-0.5x}$HIP

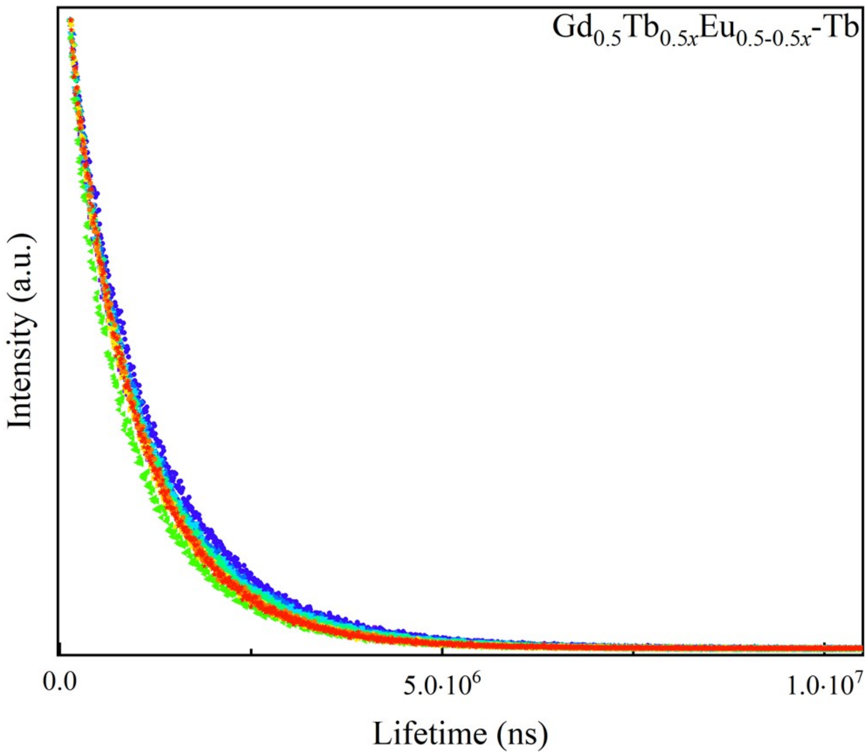

Fig. S12 The luminescent lifetime decay curves of Tb^{3+} for $Gd_{0.5}Tb_{0.5x}Eu_{0.5-0.5x}$HIP

Table S3 The overall photoluminescent quantum yields (ϕ_{Ln}^{Ligand}), and transitions determined for corresponded compounds.

Compound	ϕ_{Ln}^{Ligand} (%)	Transitions
$Gd_{0.5}Tb_{0.5}HIP$	11.68(1)	$^5D_4 \rightarrow ^7F_{6-0}$
$Gd_{0.1}Tb_{0.9}HIP$	8.46(1)	$^5D_4 \rightarrow ^7F_{6-0}$
Gd0.5Tb0.4Eu0.1HIP-Tb	11.48(1)	$^5D_4 \rightarrow ^7F_{6-0}$
$Gd_{0.5}Eu_{0.5}HIP$	11.42(1)	$^5D_0 \rightarrow ^7F_{0-6}$
$Gd_{0.1}Eu_{0.9}HIP$	6.86(1)	$^5D_0 \rightarrow ^7F_{0-6}$
Gd0.5Tb0.4Eu0.1HIP-Eu	10.91(1)	$^5D_0 \rightarrow ^7F_{0-6}$
$Gd_{0.9}Dy_{0.1}HIP$	1.33(1)	$^4F_{9/2} \rightarrow ^6H_{15/2,9/2-5/2}$
$Gd_{0.5}Dy_{0.5}HIP$	0.81(1)	$^4F_{9/2} \rightarrow ^6H_{15/2,9/2-5/2}$

Table S4 The lifetime (τ) value of Tb^{3+} in $Gd_{0.5}Tb_{0.5x}Eu_{0.5-0.5x}HIP$ alloy and corresponded energy transfer efficiency (η)

x	Tb^{3+} τ (ms)	η
0.1	0.69(1)	0.35
0.2	0.67(2)	0.36
0.3	0.67(1)	0.37
0.4	0.66(1)	0.38
0.5	0.65(1)	0.39
0.6	0.63(1)	0.41
0.7	0.59(1)	0.44
0.8	0.55(1)	0.48
0.9	0.52(1)	0.51

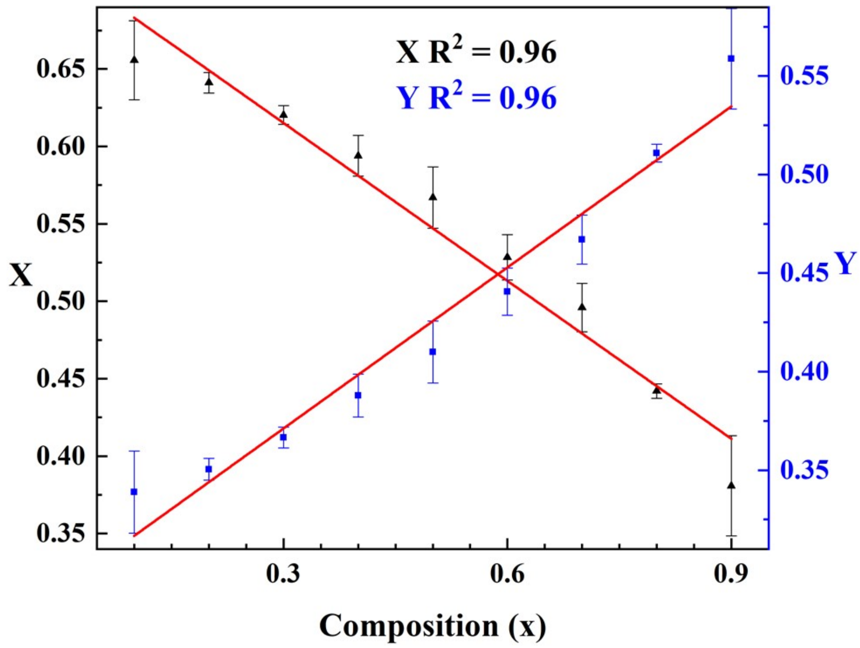

Fig. S13 Linear relationship of colormetric coordinates versus x for molecular alloy $Gd_{0.5}Tb_{0.5x}Eu_{0.5-0.5x}HIP$.

Table S5 Working ranges (K), relative sensitivity values (Sre) and ratiometric luminescent lanthanide-based MOF thermometers.

Luminescent MOF	Range (K)	Sre (% K-1)	Ref.
$Eu_{0.0069}Tb_{0.9931}$-DMBDC	50-200	1.15	1
$Tb_{0.9}Eu_{0.1}PIA$	100-300	3.27	2
$Tb_{0.99}Eu_{0.01}PIA$	100-300	2.75	2
$Tb_{0.95}Eu_{0.05}PIA$	100-250	2.48	2
$Tb_{0.50}Eu_{0.50}PIA$	75-275	2.02	2
$Tb_{0.957}Eu_{0.043}cpda$	40-300	16.0	3
$[Tb_{0.98}Eu_{0.02}(OA)_{0.5}(DSTP)]\cdot 3H_2O$	77-275	2.40	4
$[Tb_{0.98}Eu_{0.02}(BDC)_{0.5}(DSTP)]\cdot 2H_2O$	77-225	2.75	4
$Eu_{0.02}Gd_{0.98}$-DSB	20-300	4.75	5
$Eu^{3+}{}_{0.5\%}/Tb^{3+}{}_{99.5\%}$@In(OH)(bpydc)	283.15-333.15	2.53	6
$Tb_{0.95}Eu_{0.05}cpna$	25-300	2.55	7
$Tb_{0.95}Eu_{0.05}bpydc$	25-300	2.59	7

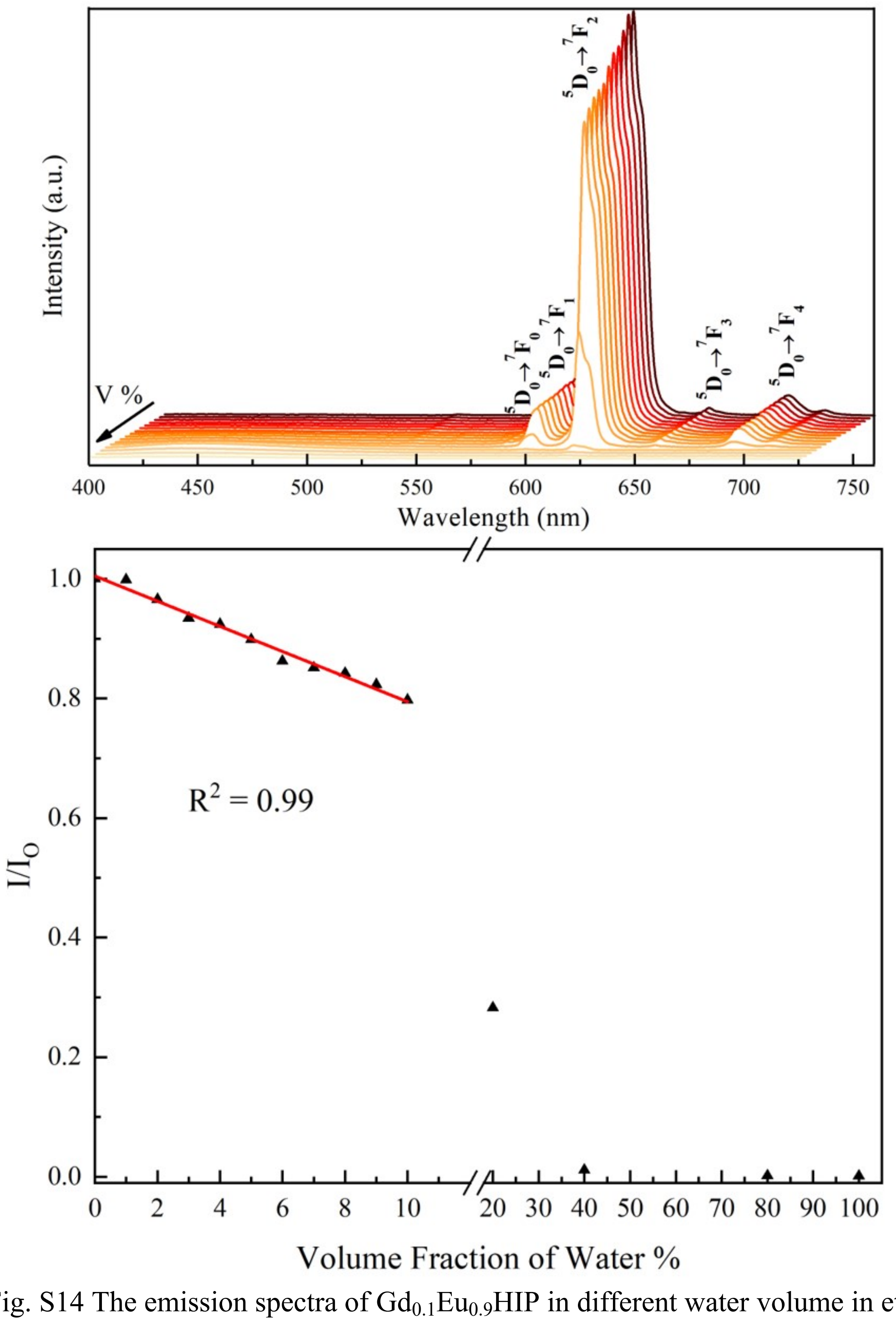

Fig. S14 The emission spectra of $Gd_{0.1}Eu_{0.9}HIP$ in different water volume in ethanol solution (top); the linear relationship of I/I_o at 613 nm versus volume fraction of water % (down).

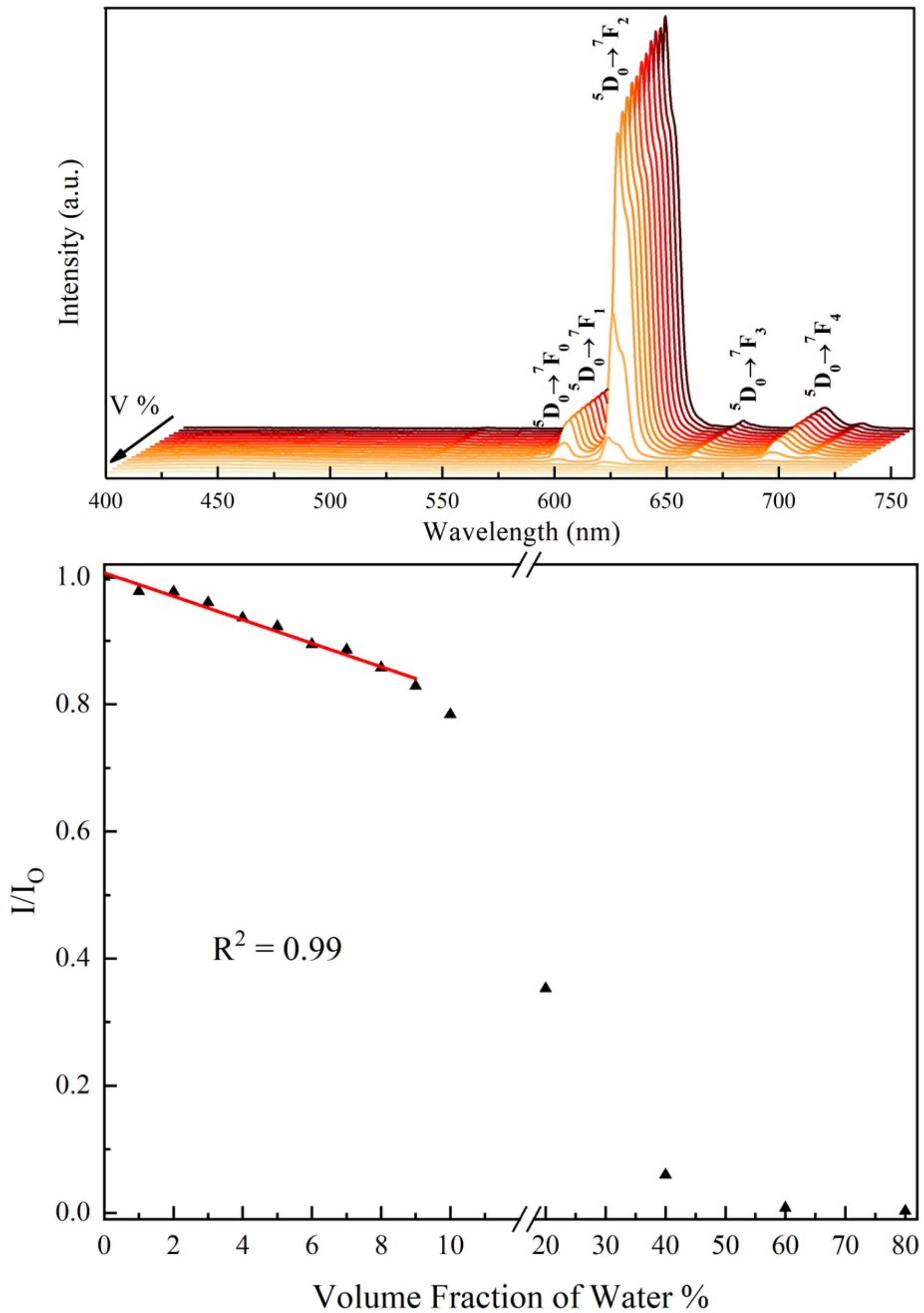

Fig. S15 The emission spectra of $Gd_{0.5}Eu_{0.5}HIP$ in different water volume in ethanol solution (top); the linear relationship of I/I_o at 613 nm versus volume fraction of water % (down).

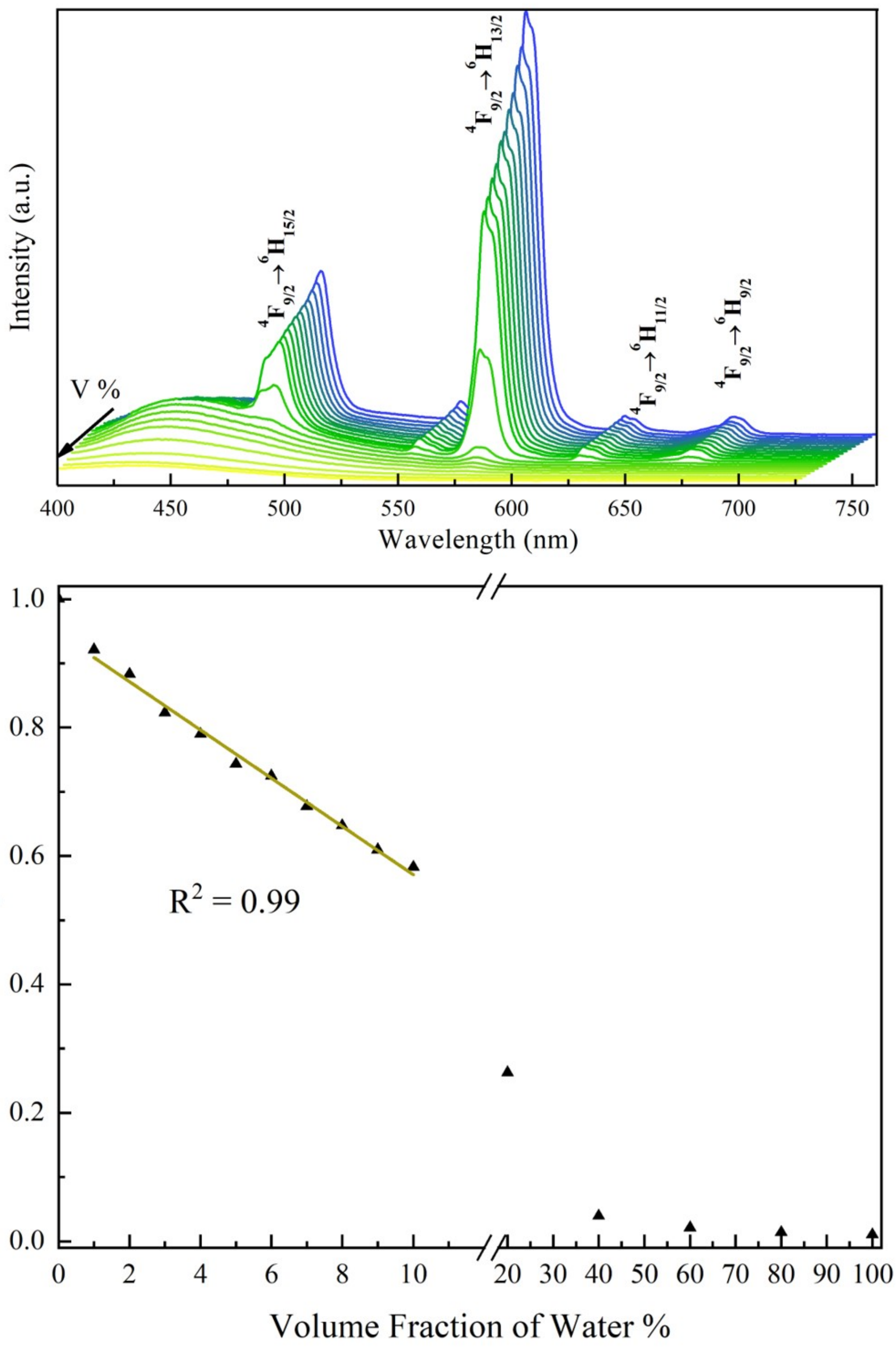

Fig. S16 The emission spectra of $Gd_{0.9}Dy_{0.1}HIP$ in different water volume in ethanol solution (top); the linear relationship of I/I_o at 571 nm versus volume fraction of water % (down).

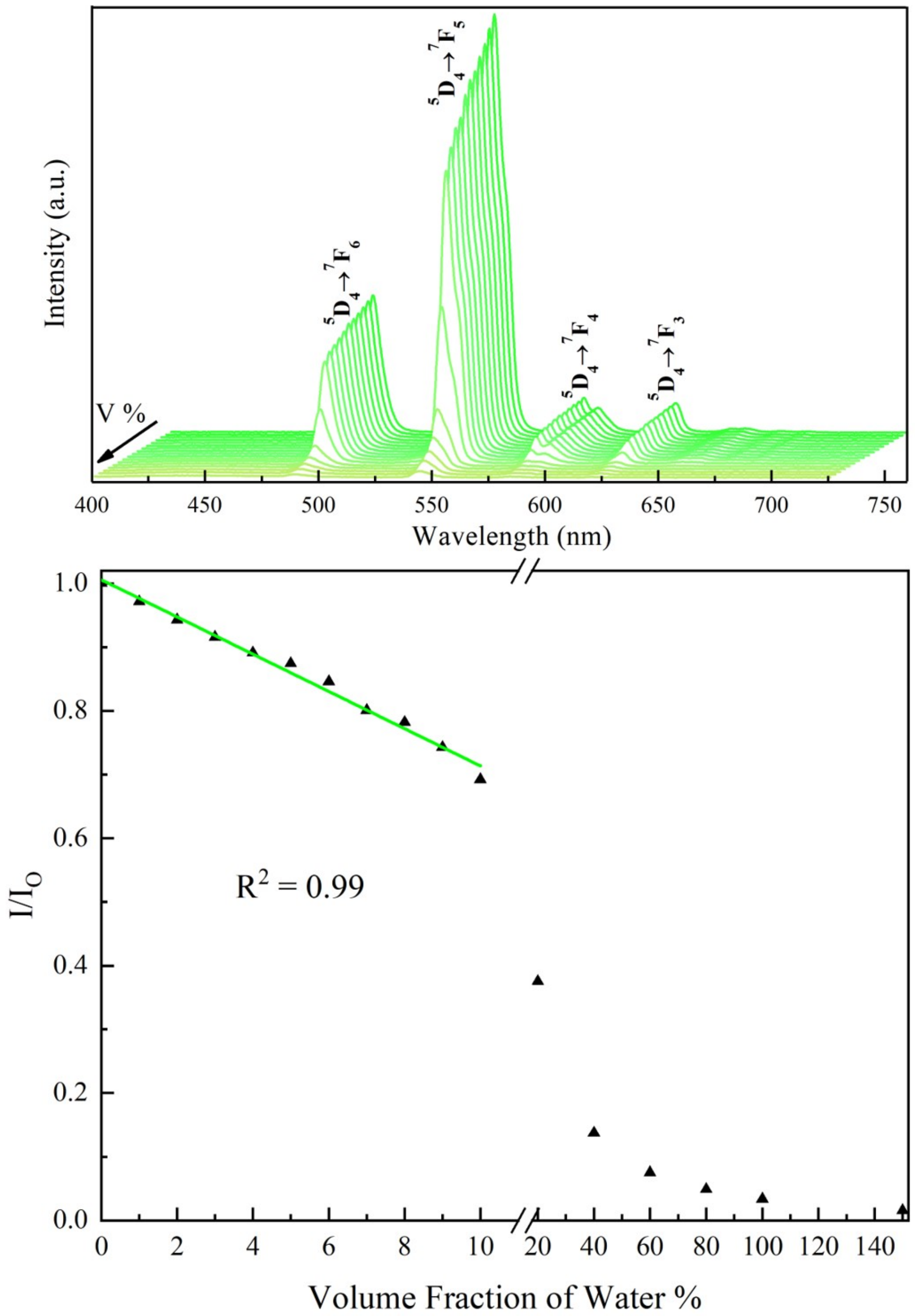

Fig. S17 The emission spectra of $Gd_{0.1}Tb_{0.9}$HIP in different water volume in ethanol solution (top); the linear relationship of I/I_o at 543 nm versus volume fraction of water % (down).

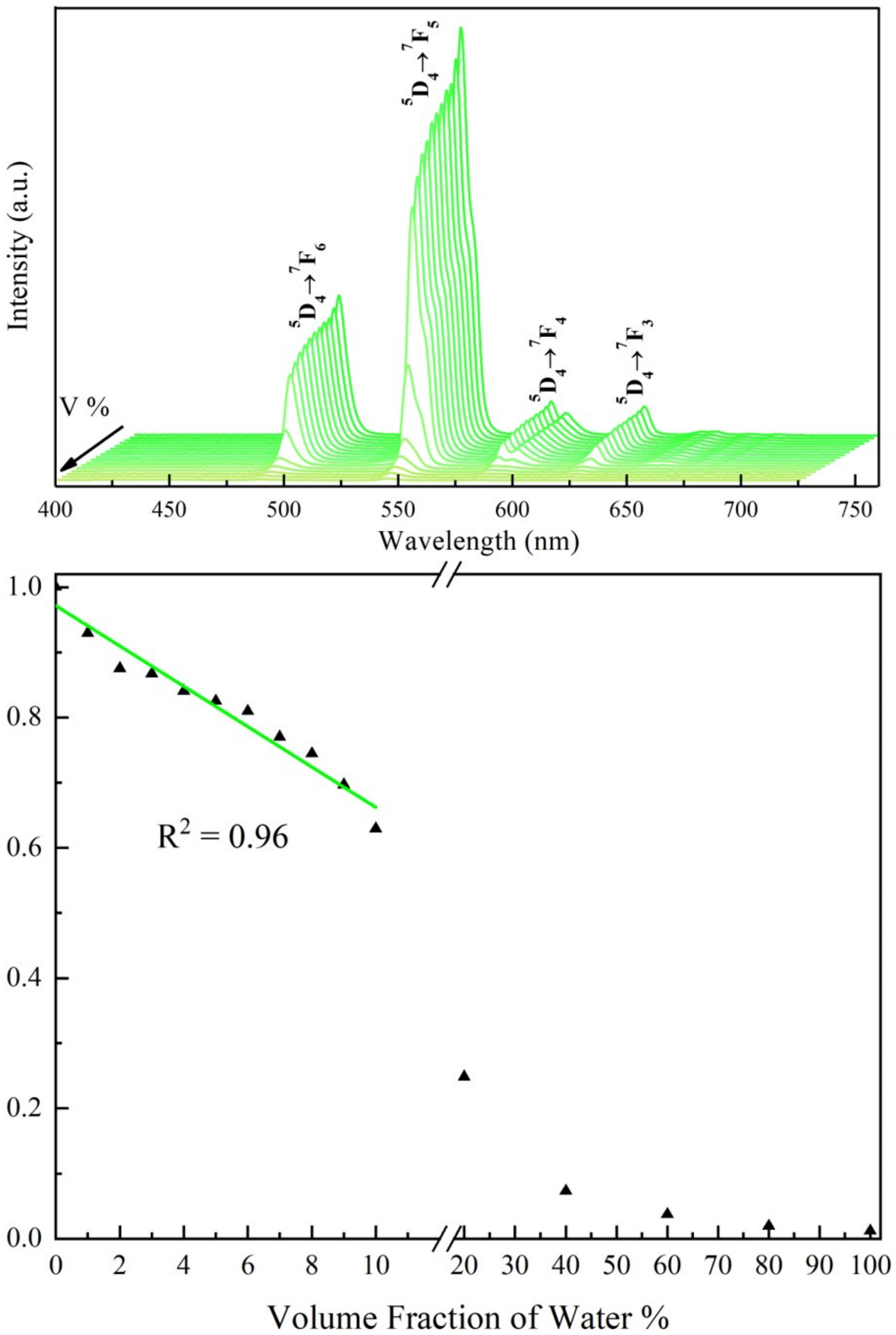

Fig. S18 The emission spectra of $Gd_{0.5}Tb_{0.5}$HIP in different water volume in ethanol solution (top); the linear relationship of I/I_o at 543 nm versus volume fraction of water % (down).

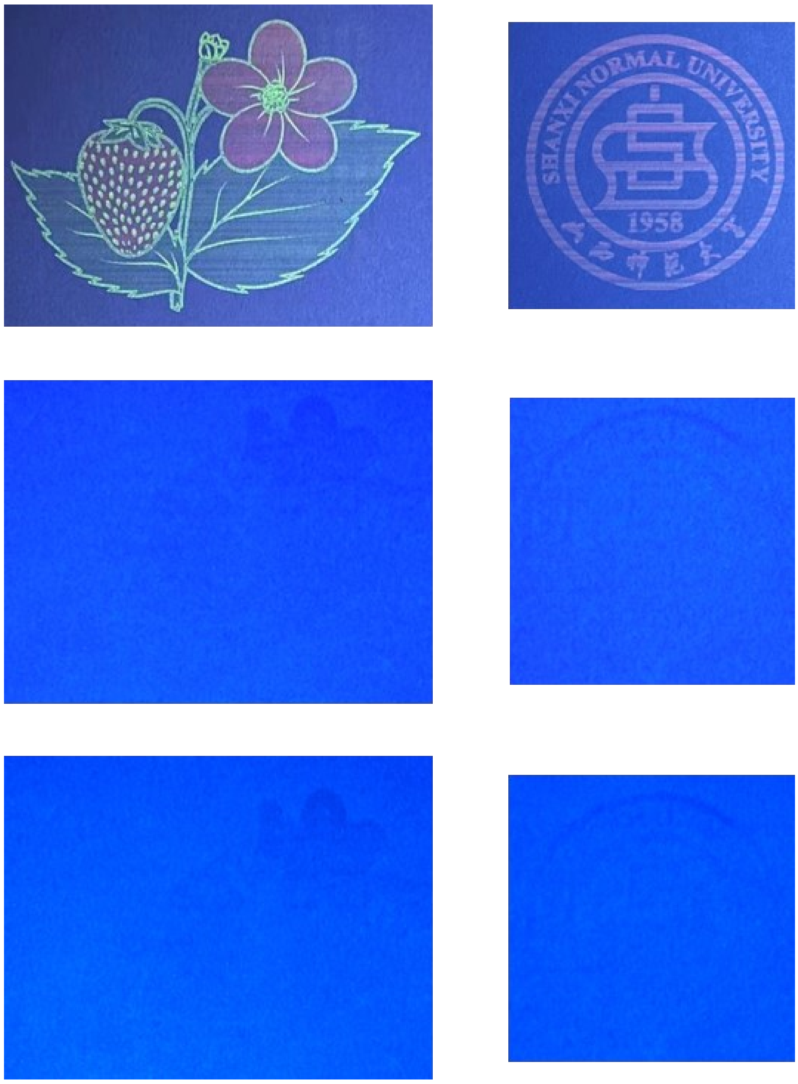

Fig. S19 The flower (left) and logo of SHANXI NORMAL UNIVERSITY (right) printed by corresponded luminescent inks and observed under UV irradiation at 312 nm (top), 365 nm (middle), 366 nm (down).

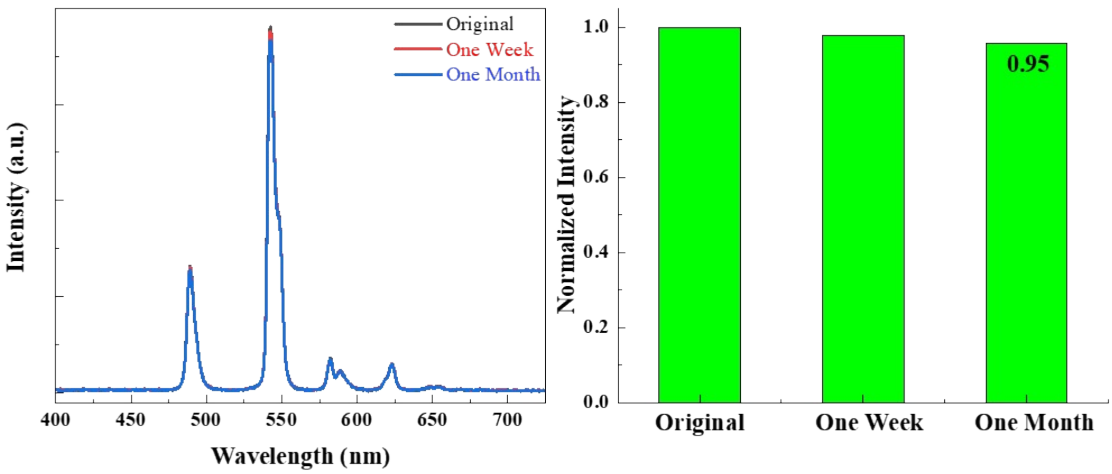

Fig. S20The emission spectra of $Gd_{0.5}Tb_{0.5}$HIP ink of original sample after one week and one month (left); corresponded normalized emission intensity at 543 nm.

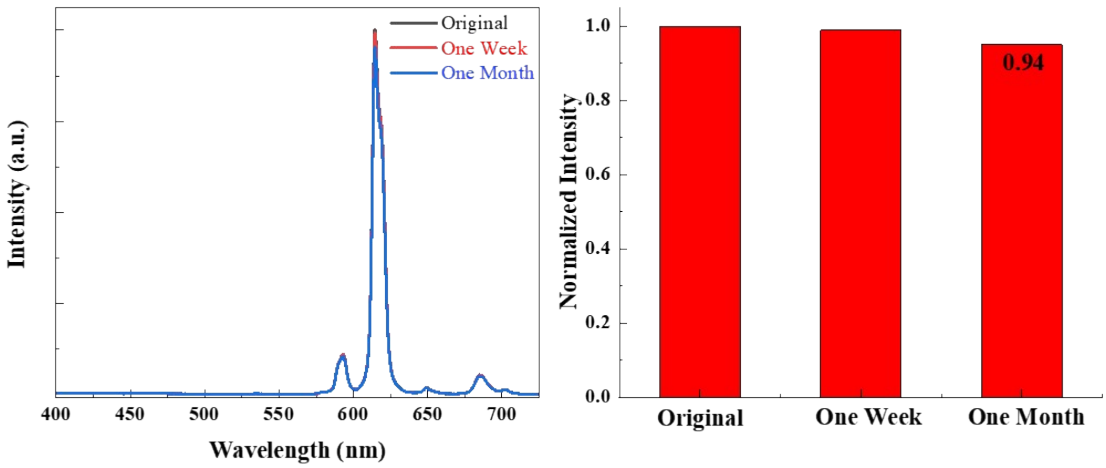

Fig. S21 The emission spectra of $Gd_{0.5}Eu_{0.5}$HIP ink of original sample after one week and one month (left); corresponded normalized emission intensity at 613 nm.

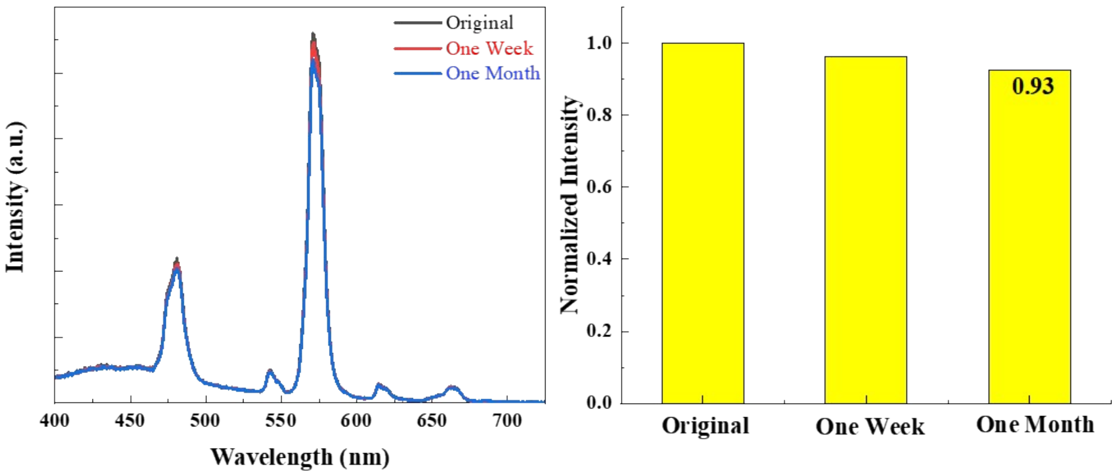

Fig. S22 The emission spectra of $Gd_{0.9}Dy_{0.1}$HIP ink of original sample after one week and one month (left); corresponded normalized emission intensity at 571 nm.

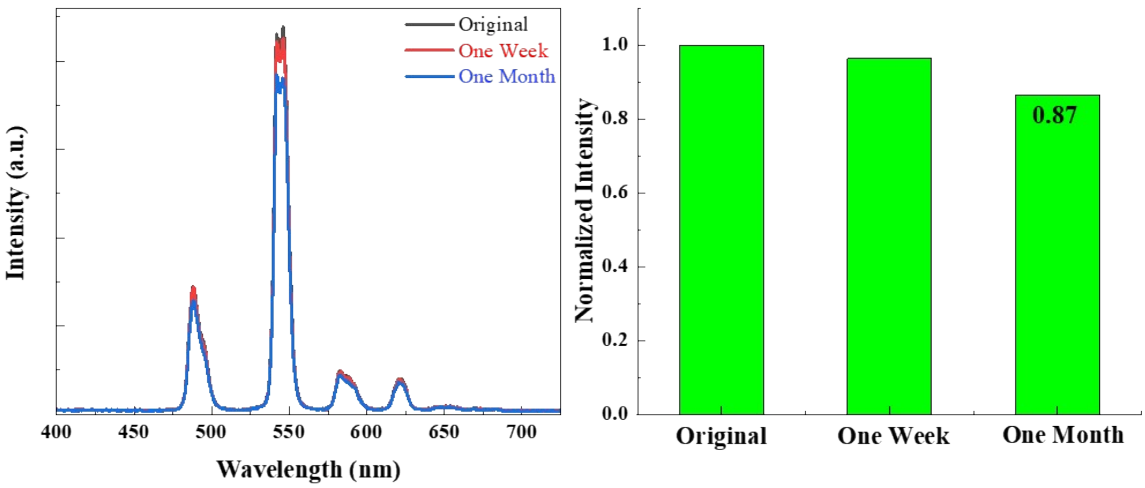

Fig. S23 The emission spectra of referenced TbMIP ink of original sample after one week and one month (left); normalized emission intensity at 543 nm.

References:

[1] Y. Cui; H. Xu; Y. Yue; Z. Guo; J. Yu; Z. Chen; J. Gao; Y. Yang; G. Qian; B. Chen, *J. Am. Chem. Soc.* **2012**, 134 (9), 3979-3982.

[2] X. Rao; T. Song; J. Gao; Y. Cui; Y. Yang; C. Wu; B. Chen; G. Qian, *J. Am. Chem. Soc.* **2013**, 135 (41), 15559-15564.

[3] Y. Cui; W. Zou; R. Song; J. Yu; W. Zhang; Y. Yang; G. Qian, *Chem. Commun.* **2014**, 50 (6), 719-721.

[4] Y. Wei; R. Sa; Q. Li; K. Wu, *Dalton. Trans.* **2015**, 44 (7), 3067-3074.

[5] R. F. D'Vries; S. Álvarez-García; N. Snejko; L. E. Bausá; E. Gutiérrez-Puebla; A. De Andrés; M. Á. Monge, *J. Mater. Chem. C* **2013**, 1 (39), 6316-6324.

[6] Y. Zhou; B. Yan; F. Lei, *Chem. Commun.* **2014**, 50 (96), 15235-15238.

[7] D. Zhao; D. Yue; K. Jiang; L. Zhang; C. Li; G. Qian, *Inorg. Chem.* **2019**, 58 (4), 2637-2644.